JOURNAL OF MAPS, 2016
http://dx.doi.org/10.1080/17445647.2016.1192330

Taylor & Francis
Taylor & Francis Group

SCIENCE

The Intra-Pontide suture zone in the Tosya-Kastamonu area, Northern Turkey

Chiara Frassi[a], Cemal M. Göncüoğlu[b], Michele Marroni[a,c], Luca Pandolfi[a,c], Leonardo Ruffini[a], Alessandro Ellero[c], Giuseppe Ottria[c] and Kaan Sayit[b]

[a]Dipartimento di Scienze della Terra, Università di Pisa, Pisa, Italy; [b]Department of Geological Engineering, Middle East Technical University, Ankara, Turkey; [c]CNR, Istituto di Geoscienze e Georisorse, Pisa, Italy

ABSTRACT

We present the first detailed geological map of the tectonic units documented in the easternmost branch of the Intra-Pontide suture (IPS) zone in the Tosya-Kastamonu area (Northern Turkey). The Main Map is at 1:50,000 scale and covers an area of about 350 km^2. It derived from 1:25,000 scale classic field mapping and represents a detailed overview of the complexities documented in the IPS zone, a tectonic nappe stack originating from the closure of the Intra-Pontide Oceanic basin and the subsequent collision between the Istanbul-Zonguldak terrane and the Sakarya composite terrane. The map shows the orientations of superposed foliations, fold axes and mineral lineations on the basis of geometric cross-cutting relationships documented within the five tectonic units of the IPS zone and provides information on its present-day architecture resulting from activity of the North Anatolian Fault.

ARTICLE HISTORY
Received 15 December 2015
Revised 9 May 2016
Accepted 17 May 2016

KEYWORDS
Metamorphic units; Intra-Pontide suture zone; Tosya-Kastamonu area; Northern Turkey

1. Introduction

The Intra-Pontide suture (IPS) zone is the northernmost ophiolite-bearing suture zone of Turkey, stretching with an east–west trend more than 400 km from Northwest to Central Turkey. It testifies to the presence of an oceanic basin, the Intra-Pontide Oceanic (IPO) basin, located between the Istanbul-Zonguldak (IZ) terrane and the Sakarya (SK) composite terrane from the Middle Triassic to the upper Paleocene (Akbayram, Okay, & Satir, 2012; Catanzariti et al., 2013; Göncüoğlu, Gürsu, Tekin, & Koksal, 2008; Robertson & Ustaömer, 2004; Şengör, Yılmaz, & Ketin, 1980; Tüysüz, 1990) (Figure 1). The convergence processes that led the closure of the IPO basin started in the Middle Jurassic and continued until the complete closure of the oceanic domain in the upper Paleocene with the building of the nappe stack. The IZ terrane, cropping out above the IPS zone, includes a Neoproterozoic crystalline basement unconformably overlain by a very thick continuous sedimentary sequence weakly deformed during the Variscan orogeny (e.g. Dean, Monod, Rickards, Demir, & Bultynck, 2000). This sequence is in turn unconformably overlain by a thick upper Permian-Paleocene sedimentary sequence including Upper Cretaceous andesite-bearing volcanoclastic sediments. The SK composite terrane (i.e. the Sakarya continent of Şengör & Yılmaz, 1981) structurally underlies the IPS zone. It is made up of a Variscan basement (Okay et al., 2014) tectonically coupled with a deformed and metamorphosed Triassic subduction/accretion complex known as the Karakaya Complex (e.g. Okay & Göncüoğlu, 2004). They are in turn covered by a non-metamorphic Lower Jurassic-Middle Paleocene sedimentary succession, whose upper part is represented by the foredeep deposits of the Tarakli Flysch (Catanzariti et al., 2013).

The IPS zone can be depicted as an imbricate stack of five tectonic units that probably derived from a wide domain including the IPO basin and its paired continental margins. Ophiolite sequences, ophiolite-bearing mélanges and metamorphic units record a complex deformation history related to the long-lived collisional-related processes affecting the southern margin of the Eurasian plate. The upper Paleocene-Eocene sedimentary deposits of the Safranbolu-Karabük Basin (e.g. Yiğitbaş, Elmas, & Yılmaz, 1999) seal the relationships among the different IPS zone units. This architecture has been affected since the upper Paleocene-Eocene by the sub-vertical strike-slip and low-angle reverse faults connected to activity of the North Anatolian Fault (NAF) (e.g. Ellero, Ottria, Marroni, Pandolfi, & Göncüoğlu, 2015).

The Central Pontides is a key area to understand both the evolution of the Eurasian continental margin during the Triassic-Cretaceous and unravel the activity of the NAF. More recently the age of metamorphism and metamorphic conditions recorded in this sector of the belt have been subject of several papers (e.g. Aygül, Okay, Oberhansli, & Ziemann, 2015; Okay et al., 2013), however no detailed geological map of the area has been published. To partly fill this gap,

CONTACT Chiara Frassi chiarafrassi@yahoo.it Dipartimento di Scienze della Terra, Università di Pisa, via S. Maria 53, 56126, Pisa, Italy

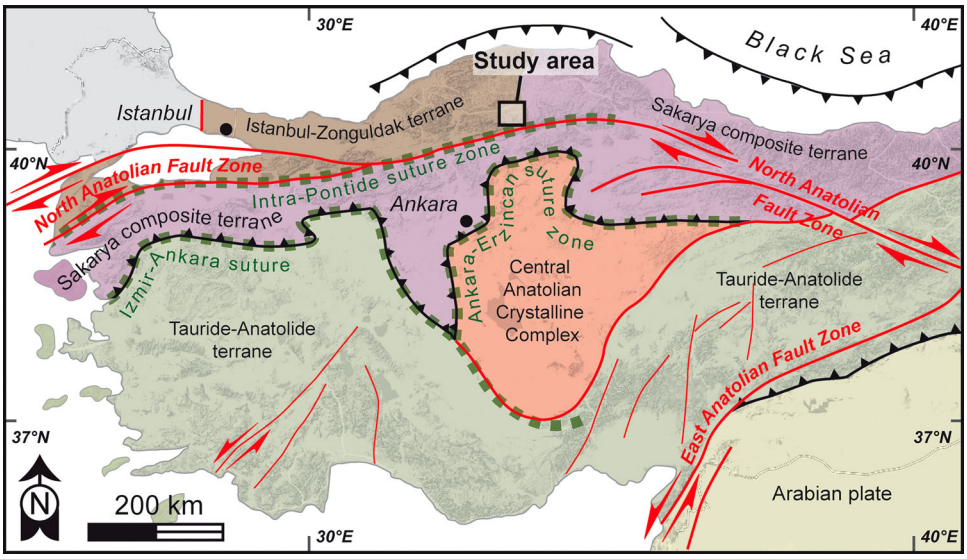

Figure 1. Geological sketch map of Anatolia and location of the study area.

we present a new 1:50,000 scale geological map of the IPS zone cropping out in the Tosya-Kastamonu area.

2. Methods

The geological units belonging to the IPS zone have been mapped according to the techniques of classic geological field survey. They have been distinguished considering the metamorphic grade. Structural elements documented in the field, namely foliations (Sn), fold axes (An) and mineral lineations (Ln), as well as bedding attitudes, are represented in the Main Map using a synoptic representation that allows to chronological differentiation of each deformation phase. To highlight their spatial orientation, each family of structural elements recognised in the field is also represented using stereographic projections (for each tectono-metamorphic unit). During fieldwork (2013–2015) we used 1:25,000 topographic maps released by the General Command of Turkey, Ankara. The same topographic maps have been reduced at 1:50,000 scale and used to draw the Main Map. The Main Map, which covers an area of nearly 350 km^2, is accompanied by a schematic structural map of the Anatolian peninsula, a tectonic sketch map of the mapped area, a geological cross-section showing the imbricate structure of the IPS zone and by stereographic projections of mesoscopic structural elements. Detailed information on the geochemistry of basic rocks cropping out in the mapped area can be found in Sayit et al. (2016).

3. IPS zone

The structural setting of the study area is characterised by an imbricate stack of tectonic units (Central Pontide Structural Complex of Tekin, Göncüoğlu, & Uzunçimen, 2012; Central Pontide Supercomplex of Okay et al., 2013) represented, from top to the bottom, by the Emirköy Unit (EMU), the Daday Unit (DDU), the Domuz Dağ Unit (DZU), the Ayli Dağ ophiolite Unit (ADU) and the Arkot Dağ Mélange (AKM) (Figure 2). The relationships among all these units are unconformably sealed by the upper Paleocene-Eocene sediments of the Tasçılar basin (Figure 3(a)) and by the Eocene fine-grained, olivine-, plagioclase- and clinopyroxene-phyric basaltic lavas (Figures 2 and 3(b)). The sediments of the Tasçılar basin are continental coarse-grained siliciclastic deposits grading to shallow marine conglomerates, arenites and fossiliferous pelites showing mixed siliciclastic-carbonatic composition. In the lowermost part of the marine deposits fossiliferous limestone can be present (cf. Safranbolu Limestone). In the southern portion of the mapped area, the stack of the tectonic units is cut by the E–W trending northern boundary of the NAF zone core (see Section 4).

The five tectonic units belonging to the IPS zone record different polyphase tectono-metamorphic evolution acquired at different times during a long-lived convergence-related process (162–102 Ma: Marroni et al., 2014; Okay et al., 2013; Figure 4). The DZU and the DDU show the more complex deformation history recording five deformation phases (D1–D5), whereas the EMU records four deformation phases. The ADU and AKM, instead, record evidence of three deformation phases. The first common deformation phase related to the building of the nappe stack produced low-angle thrusts and associated folds (i.e. D3 in DZU and DDU, D2 in EMU, D1 in ADU and AKM; see Figure 4). Lately, the five tectonic units were affected by folds with rounded hinges and sub-horizontal axial planes associated with extensional cataclastic zones (i.e. D4 in DZU and DDU, D3 in EMU, D2 in ADU and AKM; see Figure 4). Finally, the tectonic stack and the discordant upper

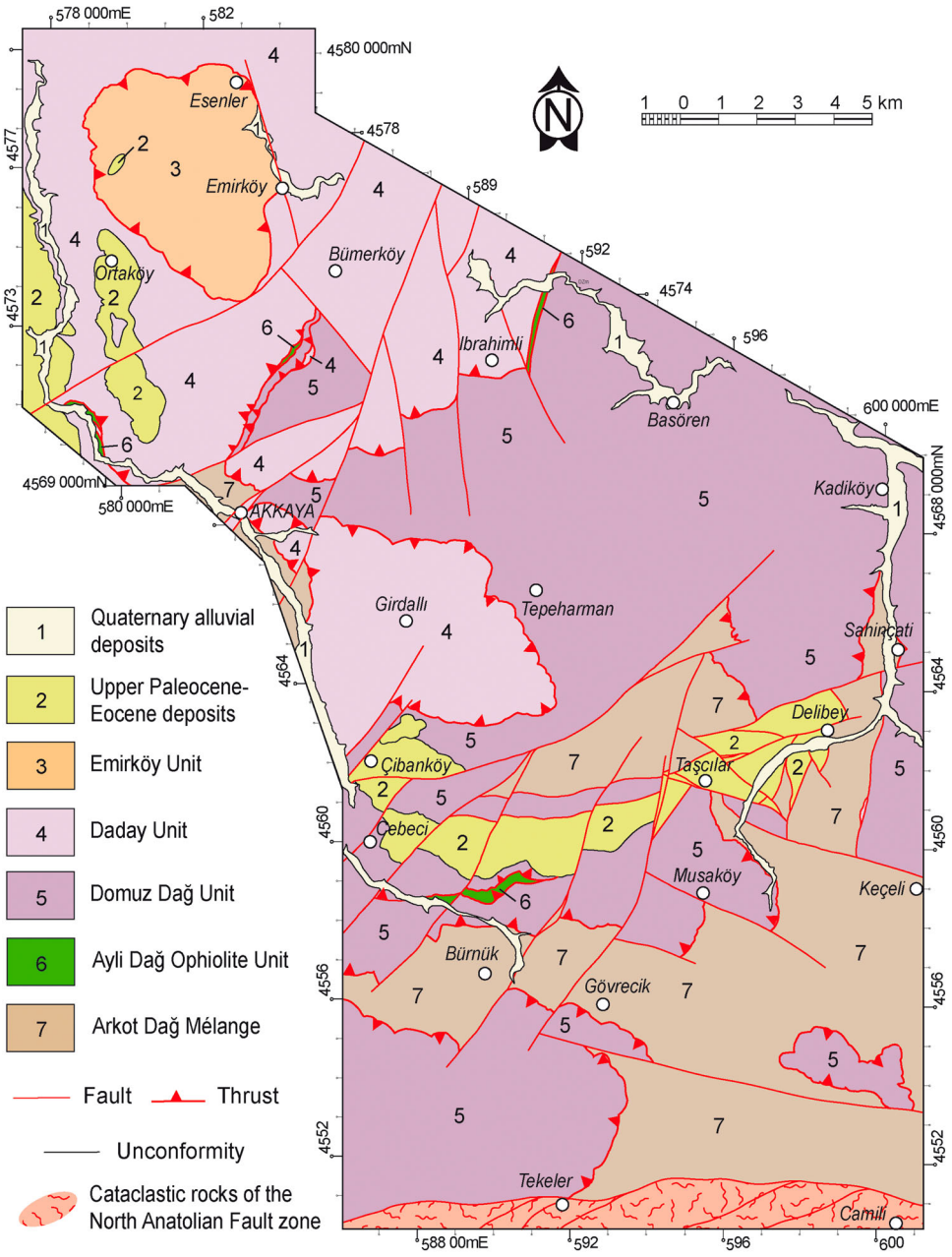

Figure 2. Tectonic sketch map of the IPS zone in the Tosya-Kastamonu area (see Figure 1 for map location).

Paleocene-Eocene deposits were affected by kilometre-scale gentle to open folds with sub-vertical axial planes and sub-horizontal axis trending E–W and by SW–NE, N–S and WNW–ESE-trending faults related to the NAF (i.e. D5 in DZU and DDU, D4 in EMU, D3 in ADU and AKM; see Figure 4).

3.1. Emirköy Unit

The EMU is represented by a ~300–400 m thick succession of metaturbidites (metapelites, metasiltstones and metarenites; EMmt in the Main Map) and subordinate metalimestones (EMmc in the Main Map). Rare F1 isoclinal folds (Figure 5(a)) with rounded and slightly thick hinges developed during the D1 deformation phase. A1 fold axes are scattered from N–S to NE–SW and dip less that 40° both towards NE and SW. F1 folds are associated with an axial plane foliation, S1, which represents the main foliation documented in the field. In metapelites and metasiltstones, S1 is a continuous foliation marked by fine-grained white micas and elongated quartz and feldspar grains (Figure 5(b)). In metarenites, S1 is marked by opaque and micaceous material deposited as a consequence of solution processes. Quartz grains are often truncated and very fine-grained micas grew in the strain shadows. Close to open F2 folds with rounded hinges related to the D2 deformation phase are the most common plicative structures detected in the field. A2 axes mainly trend NW–SE and plunge generally less than 45° both to NW and SE. The S2 axial plane foliation is a discrete and rough cleavage striking WNW–ESE that is steeply inclined both towards NE and SW. It is marked by thin, irregular and

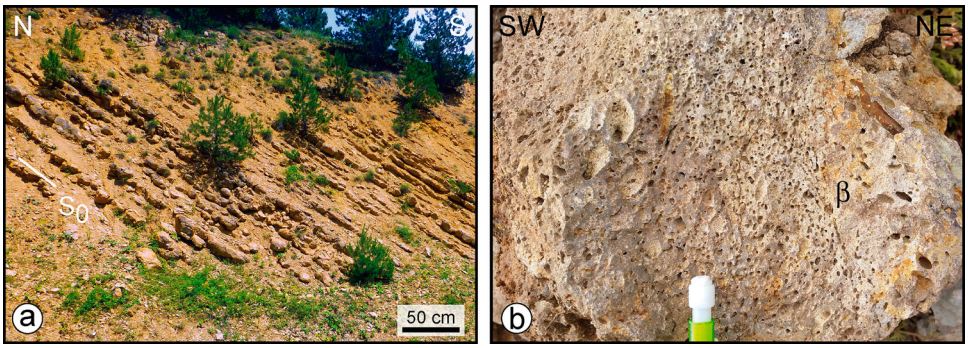

Figure 3. (a) upper Paleocene-Eocene deposits cropping out along the Tosya-Kastamonu road (S0: stratigraphic bedding); (b) vesicular basaltic lavas (β) cropping out NE of Çıbanköy village.

unit	deformation phase				
	Sp-1 S0	Sp	N S Sp	NW SE Sp	N S Sp (map scale)
Eocene					***D1 def. phase*** F1 Flt
AKM			***D1 def. phase*** S1 F1 T1	***D2 def. phase*** S2 F2 eSZ2	***D3 def. phase*** F3 Flt
ADU			***D1 def. phase*** S1 F1 T1	***D2 def. phase*** S2 F2 eSZ2	***D3 def. phase*** F3 Flt
EMU		***D1 def. phase*** S1 F1	***D2 def. phase*** S2 F2 T2	***D3 def. phase*** S3 F3	***D4 def. phase*** F4 Flt
DDU	***D1 def. phase*** S1 F1	***D2 def. phase*** S2 F2	***D3 def. phase*** S3 F3 T3	***D4 def. phase*** S4 F4 eSZ4	***D5 def. phase*** F5 Flt
DZU	***D1 def. phase*** S1 F1	***D2 def. phase*** S2 F2	***D3 def. phase*** S3 F3 T3	***D4 def. phase*** S4 F4 eSZ4	***D5 def. phase*** F5 Flt

Figure 4. Deformation history documented in the upper Paleocene-Eocene deposits and in the five tectonic units belonging to the IPS zone. The tectonic units are listed following the probable original nappe emplacement as suggested by Sayit et al. (2016). Top-to-the S thrust developed during the D3 deformation phase in the DZU and DDU the D2 deformation phase in the EMU and the D1 phase in the AKM and ADU produced the nappe stack. Deformation phases that occurred earlier may not be coeval. EMU: Emirköy unit; DDU: Daday Unit; DZU: Domuz Dağ Unit; ADU: Ayli Dağ Ophiolite Unit; AKM: Arkot Dağ Mélange. S0: bedding; S1: S1 foliation; F1: F1 fold; T1: thrust D1; S2: S2 foliation; F2: F2 fold; T2: Thrust D2; eSZ2: extensional shear zone D2; S3: S3 foliation; F3: F3 fold; T3: Thrust D3; eSZ3: extensional shear zone D3; S4: S4 foliation; F4: F4 fold; eSZ4: extensional shear zone D4; F5: F5 fold; Flt: high-angle fault of the NAF; Sp: main foliation in the field; Sp-1: relicts foliation documented in microlithons.

discontinuous films made by opaque minerals and oxides (Figure 5(b)). Rare cm-thick compressive shear zones (T2 in Figure 4) highlighted by foliated cataclasites trending approximately E–W and showing a top-to-the S shear sense developed during the D2 phase. The D3 phase produced open F3 folds with rounded hinges and sub-horizontal axial planes (Figure 5(c)) and a S3 foliation highlighted by fractures. The A3 axes show a widespread trend that range from NW–SE to SW–NE and dip mainly towards N. The D4 phase has been documented only at the map scale. It produced kilometre-scale open folds with sub-vertical axial planes and ~ E–W trending axes.

3.2. Daday Unit

The DDU (partially corresponding to the Esenler Unit of Aygül et al., 2015) is a ~400–500 m thick tectonic unit represented by a metasedimentary sequence (fine-grained micaschists, paragneisses, quartzites, metaradiolarites – DDms in the Main Map – and fine-grained marbles – DDma in the Main Map) and by bodies of fine-grained actinolite-bearing schists (DDmb in the Main Map; Figure 5(d)) that display E-MORB-, OIB-, BABB- and IAT-type signatures (Sayit et al., 2016). It has been affected by greenschist facies metamorphism overprinting an earlier

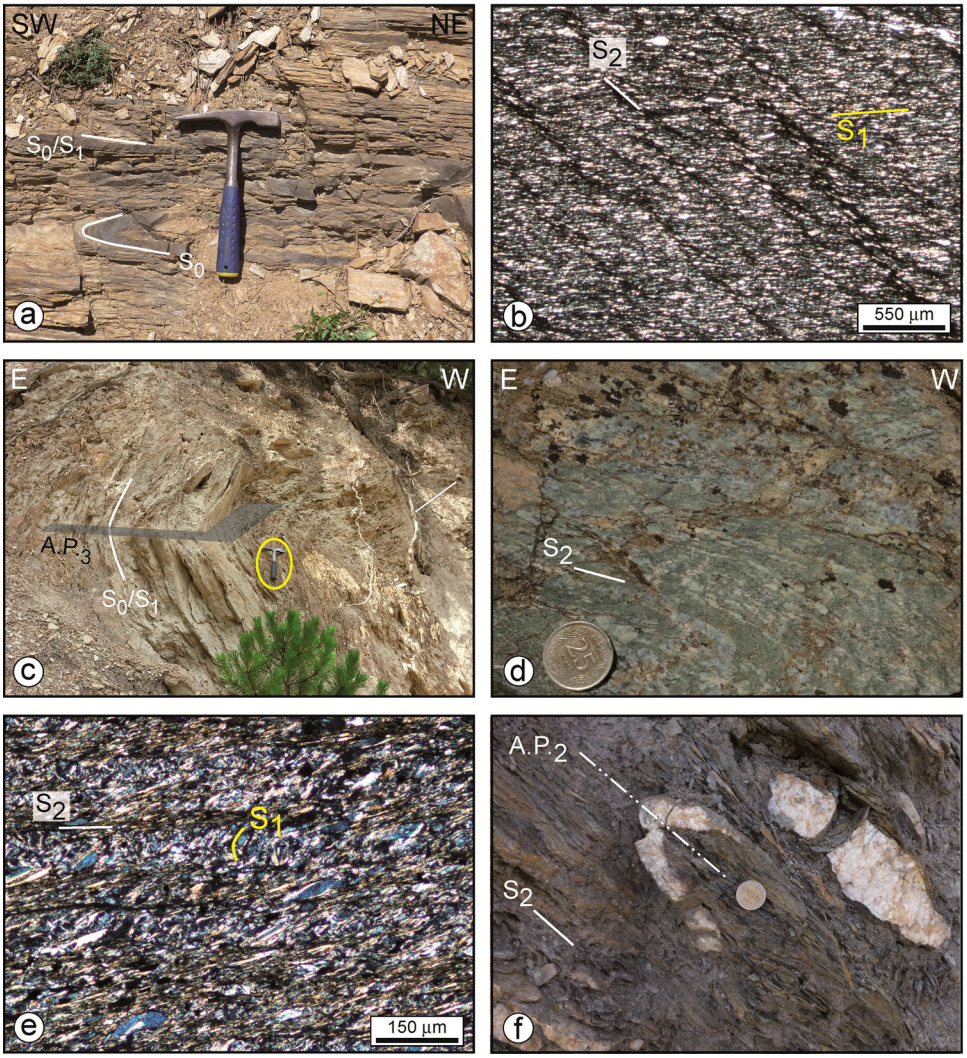

Figure 5. (a) Isoclinal F1 fold in the EMU (S0: bedding; S1: S1 foliation); (b) Photomicrograph showing the relationship between S1 and S2 foliations in the EMU. S1 foliation is a continuous foliation marked by opaque and micaceous material deposited as a consequence of solution processes. S2 is a spaced, rough, crenulation cleavage marked by opaque minerals and oxides along dissolution surfaces; (c) F3 folds with sub-horizontal axial plane (A.P.3) in the EMU (S0: bedding; S1: S1 foliation); (d) Metabasites from the DDU (S2: S2 foliation); (e) Photomicrograph showing relicts of S1 foliation preserved within D2 microlithons in the DDU. S2 foliation is marked by a discrete crenulation cleavage with rough to smooth cleavage domains marked by irregular and discontinuous dark seams of oxides and insoluble materials along dissolution surfaces; (f) F2 fold highlighted by quartz vein in micaschists form the DDU (S2: S2 foliation; A.P.2: axial plane of F2 fold).

metamorphic assemblage typical of low blueschist facies metamorphic conditions.

Relicts of the D1 phase have been documented at microscopic scale within D2 microlithons. The S1 foliation is marked by white mica (60–80 µm), elongated quartz and feldspar grains and oxides oriented orthogonal to the external foliation (Figure 5(e)). S2 foliation and tight to isoclinal F2 folds, showing thickened hinges, strongly thinned and boudinated limbs and sub-rounded up to sub-angular hinge geometry (Figure 5(f)) are the main structures produced during the D2 deformational phase. A2 axes trend N–S and NE–SW and variably plunge from sub-vertical to sub-horizontal. The S2 foliation, the main foliation documented in the field, is an axial plane foliation that strikes from NE–SW to NW–SE with extremely variable dip. In fine-grained quartz-rich micaschists and paragneisses, it is generally a continuous foliation highlighted by very fine-grained muscovite, quartz, albite, chlorite, rare chloritoid and oxides. In impure marble and fine-grained micaschist, it is a discrete crenulation cleavage with rough to smooth cleavage domains marked by irregular and discontinuous dark seems of oxides and insoluble materials along dissolution surfaces (Figure 5(e)). In metabasites, the S2 foliation is marked by lepidoblastic layers of chlorite, actinolite and epidote and granoblastic layers of elongated albite grains, enclosing fine Na-amphibole needles. Calcite and quartz are accessory phases. Mineral assemblage in fine-grained impure marble is calcite ± muscovite.

The D3 phase is characterised by open to tight cylindrical F3 folds, showing a symmetrical profile and sub-angular to sub-rounded hinge zones. A3 axes trend NW–SE shallowly plunging both towards NW

and SE. The S3 axial plane foliation is a spaced foliation striking from E–W to NW–SE and generally dipping less that 30° towards N and SW. At microscopic scale, S3 foliation is marked by rough to smooth cleavage domains highlighted by thin films of opaque minerals and oxides along dissolution surfaces. F3 folds are related to ~WNW–ESE-trending thrusts (T3 in Figure 4) dipping from 20° to 60° towards north associated with cm-thick brittle shear zones pointing to top-to-the S shearing. The D4 phase produced very open to gentle F4 folds with sub-horizontal axial planes and shallowing plunging A4 axes variably trending from NW–SE to W–E and plunging less than 20° towards E and NW. The S4 foliation is highlighted mainly by fractures. Associated with the F4 folds, extensional brittle shear zones (eSZ4 in Figure 4) reactivated the pre-existing D3 thrusts indicating a top-to-the NW sense of shear. As for the D4 deformational phase in the EMU, the D5 deformational phase has been documented only at the map scale. It produced open to gentle F5 folds with ~E–W trending sub-horizontal axes and sub-vertical axial plane.

3.3. Domuz Dağ Unit

The DZU, corresponding to the Domuzdağ Complex of Okay et al. (2006, 2013) and Aygül et al. (2015) is a ~800–1200 m thick assemblage of micaschists and impure quartzites (DDms in the Main Map; Figure 6 (a)), minor bodies of coarse-grained marbles (DZma in the Main Map) and mafic rocks (DDam in the Main Map) preserving relicts of blueschist and amphibolite facies metamorphism. Several kilometres east of the study area, metaserpentinites with boudins of eclogites retrogressed to blueschist facies have been reported by Okay et al. (2006, 2013). According to Sayit et al. (2016), the amphibolites display E-MORB, OIB-, BABB- and IAT-type signatures as those from

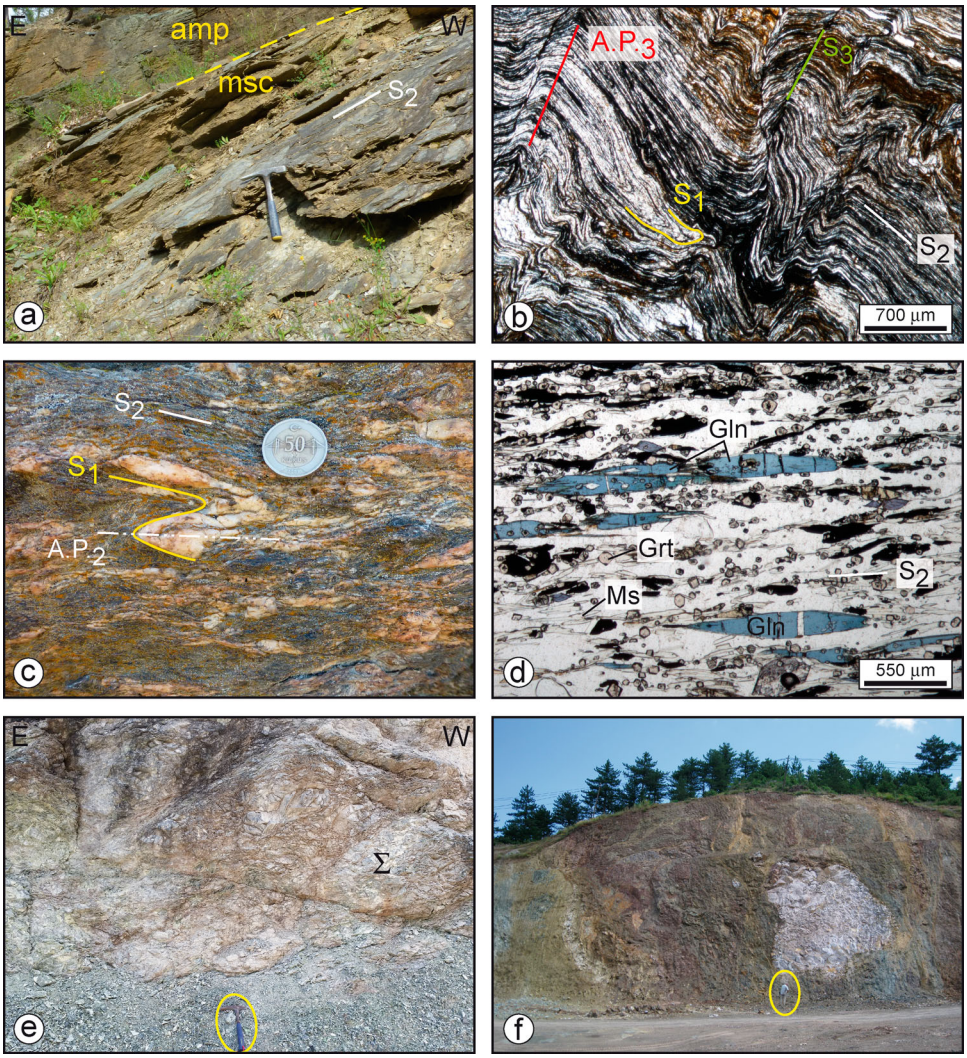

Figure 6. (a) Typical outcrop of micaschists (msc) and amphibolites (amp) in the DZU. The S2 foliation is the main foliation documented in the field; (b) Photomicrograph showing the geometrical relationship between D1, D2 and D3 structural elements in the DZU. (S1: S1 foliation; S2: S2 foliation; A.P.3: F3 axial plane); (c) Cm-sized F2 folds with axial planes (A.P.2) parallel to the main foliation documented in the field DZU; (S1: S1 foliation; S2: S2 foliation); (d) Photomicrograph of glaucophane crystals (Gln) elongated parallel to the S2 foliation (S2) preserved in lenses and/or boudins in the DZU (Ms: muscovite; Grt: garnet); (e) typical outcrop of strongly tectonized serpentinites (Σ) of the ADU; (f) Outcrop of AKM close to Kastamonu.

the DDU. Relics of the D1 phase have been occasionally documented both at micro- and mesoscopic scale. In micaschists, the S1 foliation is preserved within D2 microlithons as white mica porphyroclasts oriented at a high-angle with respect to the external S2 foliation or as rare isoclinal F2 folds (Figure 6(b)). The S2 foliation represents the main structural element documented in the field (Figure 6(a)). It is an axial plane foliation associated with rootless and intrafoliar F2 folds showing acute and thickened hinge zones and thinned limbs often affected by boudinage, necking and pinch-and-swell structures (Figure 6(c)). Micaschists and impure quartzites show a primary parageneses of quartz + feldspar + biotite + muscovite ± garnet ± staurolite that is locally retrogressed to quartz + albite + muscovite + chlorite schists. In micaschists, S2 foliation is generally defined by elongate granoblastic quartz-feldspar aggregates alternating with lepidoblastic layers made up by mm-size white mica fishes and small biotite crystals (generally strongly replaced by biotite). Relicts of garnet grains occur, embedded both by granoblastic and lepidoblastic layers. Coarse-grained amphibolites are associated with retrograded zones of albite + epidote + chlorite + actinolite schists with relict Na-amphibole and boudins of poorly re-equilibrated eclogites and garnet + rutile + Na-amphibole-bearing schists (Figure 6(d)). HT-LP metamorphism relicts have been dated at *c.* 112–100 Ma (Aygül et al., 2015; Okay et al., 2013). Impure marbles show a mineral assemblage of calcite + muscovite + biotite ± epidote ± rutile ± apatite ± titanite. The A2 fold axes show a scattered trend, ranging from NNW–SSE to NE–SW with a gentle dip both towards north and south. At the mesoscale, D2 structures are deformed by the F3 close to open folds with rounded to sub-rounded hinges and A3 fold axes trending from NW–SE to NE–SW with variable plunge both towards north and south. The F3 folds are associated with a spaced S3 convergent fanning axial plane foliation that can be classified as a crenulation cleavage in the micaschists and as disjunctive cleavage in the more competent lithologies (i.e. marbles). The S3 foliation is steeply inclined both towards east and west with predominantly N–S/NW–SE strikes. At the microscopic scale it can be classified as a spaced gradational crenulation cleavage. Occasionally, the S3 foliation is highlighted by thin films of opaque minerals and oxides along dissolution surfaces (Figure 6(b)). Metre-thick shear zones highlighted by foliated cataclasites showing a main top-to-the-S shear sense developed during the D3 phase (T3 in Figure 4). The following D4 phase is represented by structures that slightly modified the former structural setting. These D4 structures are represented by open and parallel F4 folds with N–S and NW–SE trending axes, sub-horizontal axial planes and an S4 foliation highlighted by fractures. Low-angle extensional shear zones (eSZ4 in Figure 4) characterised by brittle structures are commonly associated with the F4 folds (Figure 4). Finally, the D5 phase is represented by wide, open F5 folds, recognised mainly at map scale characterised by sub-horizontal axes trending E–W. On the whole, the tectono-metamorphic features of the DZU suggest that it formed as a subduction-related tectonic mélange (Okay et al., 2006, 2013; Sayit et al., 2016).

3.4. Aylı Dağ ophiolite Unit

Serpentinized peridotites (Figure 6(e)) with bands of dunites and pyroxenites (ADsp in the Main Map) crop out as thin slices less than 200–300 m thick along SW–NE vertical faults and along the S-verging thrusts. They have been assigned to the Ayli Dağ Unit (Göncüoğlu et al., 2012) and according to Göncüoğlu et al. (2012, 2014) and Sayit et al. (2016), they represent fragments of back-arc type oceanic lithosphere of Middle Jurassic age. These ophiolites recorded three events of deformation (Figure 4). Serpentinized peridotites are deformed by S-verging thrusts (D1 phase) that are lately reactivated as an extensional shear zone (D2 phase). Finally, they are deformed by wide to open km-scale folds with a sub-vertical axial plane and sub-horizontal axes trending E–W (D3 phase). They are not affected by orogenic metamorphism.

3.5. Arkot Dağ melange

The AKM (AKme in the Main Map; corresponding to the Kirazbaşı Complex of Aygül et al., 2015) is a late Santonian chaotic sedimentary deposit consisting of a succession where slide-blocks of different sizes and lithologies are enclosed in a sedimentary matrix consisting of shales, coarse-grained sandstones, pebbly mudstones and pebbly sandstones (Göncüoğlu et al., 2014 and references therein; Figure 6(f)). The slide-blocks, from several metres to hectometres in size, are represented by metamorphic rocks (mainly micaschists and gneisses), by ophiolites (peridotites, gabbros, basalts and cherts) and by sedimentary rocks (cherts, neritic and pelagic limestones, marly limestones and ophiolite-bearing turbidites). The geochemical analyses indicate the occurrence of N-MORB- and IAT- to BABB- basalts (Sayit et al., 2016). The thickness of the AKM cannot be estimated, but it is more than 400–500 m. The AKM is affected by a polyphase deformation (Figure 4) acquired at shallow structural levels (Göncüoğlu et al., 2014). The first deformation phase (D1) is characterised by a strong strain partitioning that produced centimetre- to decimetre-thick foliated cataclasites pointing to a top-to-the S sense of shear. They developed under very-low grade metamorphism at the boundary between mélange slices and matrix. The second deformation phase (D2) has been rarely

documented. During this phase the D1 thrusts and shear zones are partly reactivated as extensional shear zones. The last deformation phase (D3) is represented by open folds with sub-vertical axial planes and axes with E–W trend.

4. NAF zone

The NAF zone is one of the most important strike-slip continental crustal-scale fault systems in the world. In the study area, the core of the NAF zone crops out in the southern portion of the study area. It is represented by a 4–5 km wide sheared zone characterised by ~ SW–NE elongated blocks bounded by anastomosed high-angle faults.

The mesoscale structural analysis allowed measurement of 132 fault planes represented almost exclusively by high-angle faults that can be subdivided into three main systems trending roughly SW–NE, N–S and WNW–ESE, respectively. According to the plunge angles of the detected slickensides, the faults are predominantly strike-slip faults. The occurrence of multi-striated fault planes indicate that the NAF activity is characterised by a complex evolution that dissects the Eocene sediments and the underlying stack of tectonic units. This geometry and kinematic reconstruction seems to corroborate the data recently documented ~30 km south of the study area (Ellero, Ottria, Sayit, et al., 2015).

5. Conclusions

This study has produced the first detailed geological and structural map of the units cropping out in the eastern part of the IPS zone in the Central Pontides, northern Turkey. The five metamorphic units belonging to the IPS zone record a different polyphase tectono-metamorphic evolution acquired at different times during the convergence-related processes that led to the closure of the IPO basin. The first common deformation phase related to the building of the nappe stack (i.e. D3 in DZU and DDU, D2 in EMU, D1 in ADU and AKM) occurred during the final stages of the IZ-SK collision. The earlier deformation phases documented in the EMU, DDU and DZU probably testify to accretion processes active during the early stages of convergence. Since the upper Paleocene-lower Eocene, the activity of the NAF dismembered the tectonic stack and the discordant deposits producing kilometre-scale gentle to open folds (F5 in DZU and DDU, D4 in EMU, D3 in ADU and AKM) and high-angle faults.

Software

The map database was built using Esri ArcGIS and the final map layout assembled using Illustrator CS5. Topographic maps were acquired from 1:25,000 scaled topographic map nr. F31 b3, F32 a3, F32 a4, F32 d1, F32 d2, F32 d3, F32 d4 from General Command of Turkey-Ankara.

Stereonet plots were produced using OSXStereonet (v. 3.5) by N. Cardozo and R.W. Allmendinger and then redrawn using Illustrator CS5.

Acknowledgements

We thank A. Zanchi, A. Traforti and J. Cron for the constructive criticisms that helped to improve the manuscript and the Main Map and C. Riccomini for the editorial work.

Disclosure statement

No potential conflict of interest was reported by the authors.

Funding

This research was supported by Darius Project and by Prin 2008 and Prin 2010–2011 projects (resp. M. Marroni).

ORCiD

Chiara Frassi http://orcid.org/0000-0002-7522-9905
Cemal M. Göncüoğlu http://orcid.org/0000-0002-4216-6995
Michele Marroni http://orcid.org/0000-0002-2947-3739
Luca Pandolfi http://orcid.org/0000-0002-6129-647X
Alessandro Ellero http://orcid.org/0000-0002-0221-8623
Giuseppe Ottria http://orcid.org/0000-0002-0797-5500
Kaan Sayit http://orcid.org/0000-0001-6859-4536

References

Akbayram, K., Okay, A. I., & Satir, M. (2012). Early Cretaceous closure of the Intra-Pontide Ocean in western Pontides (northwestern Turkey). *Journal of Geodynamics*, *65*, 38–55.

Aygül, M., Okay, A. I., Oberhansli R., & Ziemann, M. A. (2015). Thermal structure of low-grade accreted Lower Cretaceous distal turbidites, the Central Pontides, Turkey: Insights for tectonic thickening of an accretionary wedge. *Turkish Journal of Earth Sciences*, *24*, 461–474.

Catanzariti, R., Ellero, A., Göncüoğlu, M. C., Marroni, M., Ottria, G., & Pandolfi, L. (2013). The Taraklı Flysch in the Boyali area (Sakarya Terrane, northern Turkey): Implications for the tectonic history of the intraPontide suture zone. *Compte Rendues des Geosciences*, *345*, 454–461.

Dean, W. T., Monod, O., Rickards, R. B., Demir, O., & Bultynck, P. (2000). Lower Palaeozoic 328 stratigraphy and palaeontology, Karadere-Zirze area, Pontus Mountains, northern Turkey. *Geological Magazine*, *137*, 555–582.

Ellero, A., Ottria, G., Sayit, K., Catanzariti, R., Frassi, C., Göncüoğlu, M. C., … Pandolfi, L. (2015). Geological and geochemical evidences for a late cretaceous continental arc in the central pontides, northern Turkey. *Ofioliti*, *40*, 73–90.

Ellero, A., Ottria, G., Marroni, M., Pandolfi, L., & Göncüoğlu, M. C. (2015). Analysis of the North Anatolian shear zone

in Central Pontides (northern Turkey): Insight for geometries and kinematics of deformation structures in a transpressional zone. *Journal of Structural Geology*, *72* 124–141.

Göncüoğlu, M. C., Gürsu, S., Tekin, U. K., & Koksal, S. (2008). New data on the evolution of the Neotethyan oceanic branches in Turkey: Late Jurassic ridge spreading in the Intra-Pontide branch. *Ofioliti*, *33*, 153–164.

Göncüoğlu, M. C., Marroni, M., Pandolfi, L., Ellero, A., Ottria, G., Catanzariti, R., … Sayit, K. (2014). The Arkot Dağ Mélange in Araç area, central Turkey: Evidence of its origin within the geodynamic evolution of the Intra-Pontide suture zone. *Journal of Asian Earth Sciences*, *85* 117–139.

Göncüoğlu, M. C., Maroni, M., Sayit, K., Tekin, U. K., Ottria, G., Pandolfi, L., & Ellero, A. (2012). The Ayli Dağ ophiolite sequence (central-northern Turkey): A fragment of middle Jurassic oceanic lithosphere within the Intra-Pontide suture zone. *Ofioliti*, *37*, 77–91. doi:10.4454/ofioliti.v37i2.407

Marroni, M., Frassi, C., Göncüoğlu, M. C., Di Vincenzo, G., Pandolfi, L., Rebay, G., … , Ottria, G. (2014). Late Jurassic amphibolite facies metamorphism in the Intra-Pontide suture zone (Turkey): An eastward extension of the vardar ocean from the Balkans into Anatolia? *Journal of the Geological Society*, *171*, 605–608.

Okay, A. I., & Göncüoğlu, M. C. (2004). The Karakaya complex: A review of data and concepts. *Turkish Journal of Earth Sciences*, *13*, 77–95.

Okay, A. I., Sunal, G., Sherlock, S., Altıner, D., Tüysüz, O., Kylander-Clark, A. R. C., & Aygül, M. (2013). Early Cretaceous sedimentation and orogeny on the active margin of Eurasia: Southern central pontides, Turkey. *Tectonics*, *32*, 1247–1271.

Okay, A. I., Sunal, G., Tüysüz, O., Sherlock, S., Keskin, M., & Kylander-Clark, A. R. C. (2014). Low-pressure-high-temperature metamorphism during extension in a Jurassic magmatic arc, Central Pontides, Turkey. *Journal of Metamorphic Geology*, *32*, 49–69.

Okay, A. I., Tüysüz, O., Satır, M., Özkan-Altıner, S., Altıner, D., Sherlock, S., & Eren, R. H. (2006). Cretaceous and Triassic subduction-accretion, HP/LT metamorphism and continental growth in the central pontides, Turkey. *Geological Society of America Bulletin*, *118*, 1247–1269.

Robertson, A. H. F., & Ustaömer, T. (2004). Tectonic evolution of the Intra-Pontide suture zone in the Armutlu Peninsula, NW Turkey. *Tectonophysics*, *381*, 175–209.

Sayit, K., Marroni, M., Göncüoğlu, M. C., Pandolfi, L., Ellero, A., Ottria, G., & Frassi, C. (2016). Geological setting and geochemical signatures of the mafic rocks from the Intra-Pontide suture zone: implications for the geodynamic reconstruction of the Mesozoic Neotethys. *International Journal of Earth Sciences*, *105*, 39–64.

Şengör, A. M. C., & Yılmaz, Y. (1981). Tethyan evolution of Turkey: A plate tectonic approach. *Tectonophysics*, *75*, 181–241.

Şengör, A. M. C., Yılmaz, Y., & Ketin, İ. (1980). Remnants of a pre-Late Jurassic ocean in northern Turkey: Fragments of Permian-Triassic Paleo-Tethys. *Geological Society of America Bulletin*, *91*, 599–609.

Tekin, U. K., Göncüoğlu, M. C., & Uzunçimen, S. (2012). Radiolarian assemblages of Middle and Late Jurassic to early late cretaceous (Cenomanian) ages from an olistolith record pelagic deposition within the Bornova Flysch zone in western Turkey. *Bulletin de la Societe Geologique de France*, *183*, 307–318.

Tüysüz, O. (1990). Tectonic evolution of a part of the Tethyside Orogenic collage: The Kargı Massif, Northern Turkey. *Tectonics*, *9*, 141–160.

Yiğitbaş, E., Elmas, A., & Yılmaz, Y. (1999). Pre-Cenozoic tectonostratigraphic components of the Western Pontides and their geological evolution. *Geological Journal*, *34*, 55–74.